

Light scattering from a dipole near a rough metallic surface

D. Agassi*

Department of Physics and Astronomy, University of Rochester, Rochester, New York 14627

(Received 8 July 1985)

We discuss the resonance fluorescence and absorption spectra pertaining to a dipole near a randomly rough metallic surface. In the framework of a fully quantum-mechanical formulation, the effects of the rough surface are embodied in the statistical properties of the matrix elements that couple surface-plasmon and reflected-wave modes. We analyze the dynamics of the system under the approximation of neglecting the diffuse photon and surface-plasmon (polariton) scattering, yet accounting for the surface-plasmon and photon coupling to all orders. We find that surface-roughness induces distortions in the flat-surface Lorentzian line shape toward a Gaussian line shape as the surface-roughness amplitude increases.

I. INTRODUCTION

Surface roughness is a generic term used to describe deviations of a real, nominally flat, surface from the idealization of a perfectly flat surface. Its existence has important effects on the surface optical properties. For example, the irregular surface geometry of spikes and nooks gives rise to the laser speckle pattern and to large local-field enhancements.¹ The latter effect is believed to underlie the observed giant enhancement in the Raman cross section of molecules deposited on such a rough surface.² Another manifestation of surface roughness is the coupling between light (photons) and surface modes, e.g., surface plasmons (SP) in the case of a metallic surface.³⁻⁶ In this sense a rough surface acts like a grating: It promotes *elastic* scattering between photons and SP quanta by providing the surface-parallel momentum mismatch. This feature has been employed, e.g., to enhance light emission from tunnel junctions,⁷⁻⁹ where the idea is to convert surface-modes excitation into light.

The details of the roughness depend on the fabrication method of the surface. These are usually ill characterized. They take forms such as large [$O(10\text{ nm})$] "pits and boulders," terraces, local defects of atomic dimensions, lines of dislocations, etc. In the context of a light probe with a wavelength much larger than a typical scattering protrusion, the distinction between the various kinds of rough surfaces is blurred. Consequently, it is natural to adopt a generic model which assumes a random surface profile distribution characterized by a few phenomenological parameters.³⁻⁶ The scattering of light from such a surface has been treated in the literature in classical terms using one of several approaches such as Green-function techniques,^{1,10,11} the separation of the surface region (selvedge) from the rest of space and parametrizing the ensuing coupling between the two,¹² employing the classical Ewald-Osean identity,¹³ and the matching of boundary conditions across the rough surface.^{3-6,14} In most of these studies, the surface-roughness amplitude is considered as small.

The present work goes one step further by considering a system comprised of a rough surface plus a nearby dipole

(Fig. 1). The focus is on interaction between the dipole and surface excitations, i.e., the manner in which surface roughness modifies light scattering by the dipole. This system occurs in a substantial body of experimental work.¹⁵ A novel feature of our approach is the following: In a fully quantum-mechanical treatment of the system the roughness-induced coupling between SP excitations and light emission or absorption is expressed in terms of matrix elements which couple the SP and photon modes. The assumed random character of the surface roughness is reflected in statistical properties of these matrix elements, and consequently the surface-roughness modeling enters via statistical assumptions [Eq. (3.5)] on these matrix elements. These statistical assumptions are consistent with, yet more general than, the well-accepted model for surface roughness.^{3-6,10,11} Our approach has several advantages. (a) It allows us to account for the SP coupling to light due to surface roughness of arbitrary amplitude, provided the diffuse light and SP scattering processes are neglected. This approximation is in keeping with the focus of this work on the dipole-SP coupling. (b) It allows us to correctly evaluate the resonance fluorescence (RF) spectrum of the dipole which mandates the use of a fully quantized theory.¹⁶ (c) It underscores the structural similarity between surface-roughness random fields (elastic scattering) and surface-generated dynamical fluctuations (inelastic scattering) treated elsewhere and in an accompanying paper.¹⁷ The latter are also referred to as the optical Johnson noise. This similarity makes it possible to simply account for the common situation where both types of fluctuations coexist (Sec. IV). (d) As will become apparent below, the quantum formalism leads to a simple, transparent formulation.

The model takes for the dipole a two-level system,¹⁶ which is the simplest configuration accommodating one natural frequency. To eliminate unnecessary complications we neglect the "diffuse" light scattering¹⁴ and SP elastic scattering by the rough surface.⁸ The former, for instance, underlies the laser speckle pattern¹⁸ which is not the issue in the present work. The system is driven by a weak, continuous, monochromatic laser, turned on abruptly at $t=0$. The metallic surface is assumed in the

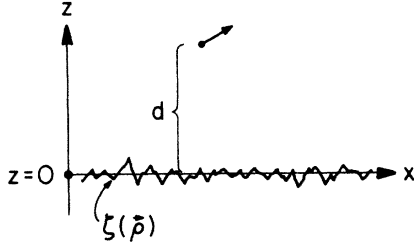


FIG. 1. The system under consideration: A dipole, indicated by an arrow, located at distance d from the $z=0$ plane. The deviations of the rough surface from the average perfectly flat surface at $z=0$ is denoted by $\zeta(\rho)$; see text.

first part of this work as lossless. This assumption is later relaxed (Sec. VI).

To evaluate the dipole RF and absorption spectra we derive and solve the Heisenberg equations of motion.¹⁶ In so doing the dynamics of the system is completely solved. One other possible application of our solution is the evaluation of the modified SP dispersion relation;^{8,19–21} however, this issue is not pursued here any further. All our results depend only on the *form* of the statistical assumptions pertaining to the SP-photon coupling matrix elements. The specifics of the surface-roughness model are lumped into the second moment of these matrix elements.

The main result of this work, besides establishing a flexible and powerful framework, is the prediction of a qualitative line-shape change as the surface-roughness-induced width γ_c is increased. This width [Eqs. (3.20) and (4.6)] depends on a combination of SP-photon coupling and the dipole-surface coupling. The line shape is approximately given by [Eq. (4.5)]

$$I(\omega) = \int_0^\infty dx \int_0^\infty dy \exp[-i(\omega - i\gamma_D)x + i(\omega + i\gamma_D)y] \times \exp(-\frac{1}{2}(x-y)^2\gamma_c^2), \quad (1.1)$$

where γ_D is the surface-renormalized dipole width. When the roughness amplitude is very small then $\gamma_c \ll \gamma_D$ and the spectral line shape (1.1) is Lorentzian. In the opposite extreme, i.e., $\gamma_c \gg \gamma_D$, expression (1.1) yields a Gaussian [Eq. (4.7)]. Crude estimates indicate that the Gaussian line-shape limit can only be approached but never fully realized. This conclusion, however, does not exclude situations where considerable line-shape distortion, given by (1.1), are present. In the particular limit of no dipole, we recover the reflectivity dip near the asymptotic SP energy.²²

The paper is organized as follows. In Sec. II we introduce the model for a lossless rough metallic surface, and the ensuing equations of motion are derived in Sec. III. Section IV is devoted to the derivation of the RF spectrum. Since the surface is lossless, the RF spectrum is particularly simple, i.e., it consists only of a Rayleigh δ peak. In Sec. V we evaluate the absorption or reflectivity spectrum, which is considerably more complex. The combination of surface roughness and the optical Johnson noise and a brief discussion are given in Sec. VI. The Appendixes contain pertinent technical details.

II. THE MODEL

The system considered (Fig. 1) consists of a dipole near a rough metallic surface and a weak, continuous driving laser turned on abruptly at $t=0$. We assume the common random roughness model for the surface's profile,^{3–6} i.e., the deviation $\zeta(\rho)$ of the actual surface from a perfectly flat one (Fig. 1) is a stochastic process as a function of the surface-parallel coordinate ρ . To simplify the analysis at this stage the surface is assumed to be lossless. This restriction is relaxed in Sec. VI. Finally, the dipole is approximated by two-level atom¹⁶ to accommodate one natural frequency.

The model is constructed in two stages. We first recap the unperturbed system model, i.e., that of a dipole near a perfectly flat surface, and then add to it the surface-roughness perturbation. Our approach is fully quantum mechanical. The unperturbed system Hamiltonian \hat{H}_0 describes the dipole interaction between the two-level system and the electromagnetic field in the presence of a perfectly flat metallic surface, treated as a jellium.^{17,23} It follows (hereafter carets denotes operators)

$$\hat{H}_0 = \hat{H}_A + \hat{H}_F + \hat{H}_{\text{int}}, \quad (2.1)$$

where the atomic Hamiltonian \hat{H}_A is

$$\hat{H}_A = E_0 |0\rangle\langle 0| + E_1 |1\rangle\langle 1| \quad (2.2)$$

with $|0\rangle$ and $|1\rangle$ denoting the atom's ground and excited states, respectively, and E_0 and E_1 the corresponding energies. The electromagnetic field-surface Hamiltonian \hat{H}_F has the standard mode decomposition⁶

$$\hat{H}_F = \sum_m \hbar\omega_m \hat{a}_m^\dagger \hat{a}_m, \quad (2.3)$$

where \hat{a}_m and \hat{a}_m^\dagger are the annihilation and creation operators, respectively, and m runs over all the relevant modes. In the present context one class of modes are the reflected-wave modes. They are specified by $\lambda = (\omega_\lambda, \mathbf{k}_\lambda, q_\lambda; i)$, where the free-space frequency is $\omega_\lambda = c(k_\lambda^2 + q_\lambda^2)^{1/2}$, \mathbf{k}_λ and q_λ are the surface-parallel and perpendicular momenta, respectively, and i assumes two polarization indices, e.g., s and p polarization. Given a quantization volume of an infinite rod in the z direction with a square cross section of area L^2 , the \mathbf{k}_λ variable is discrete and q_λ is continuous. The other class of modes m are the SP specified by $m = (\mathbf{k}_\parallel; i)$ where \mathbf{k}_\parallel denotes the surface-parallel momentum component, again quantized in a square of area L^2 . For a one-interface configuration, only p -polarization SP modes are admissible. In the sequel we always omit the polarization index in conjunction with SP to avoid cumbersome notation. Finally, the interaction dipole term \hat{H}_{int} has been evaluated elsewhere,¹⁷ and has the form

$$\hat{H}_{\text{int}} = \sum_m (\hbar\Omega_m \hat{a}_m^\dagger \hat{B} + \hbar\Omega_m^* \hat{B}^\dagger \hat{a}_m). \quad (2.4)$$

In (2.4) the dipole operator is defined by $\hat{B} = |0\rangle\langle 1|$, and the coupling matrix elements Ω_m depend on the dipole distance from the surface d (Fig. 1).

Surface roughness couples the flat-surface reflected-

waves modes and SP modes by providing the momentum mismatch between the two. Consequently, the full model Hamiltonian \hat{H} is (Fig. 2)

$$\hat{H} = \hat{H}_0 + \sum_{\mathbf{k}_{||}, \lambda} [\hbar V_e(\mathbf{k}_{||}, \lambda) \hat{a}_{\lambda}^{\dagger} \hat{a}_{||} + \hbar V_e^*(\mathbf{k}_{||}, \lambda) \hat{a}_{||}^{\dagger} \hat{a}_{\lambda}], \quad (2.5)$$

where the matrix element $V_e(\mathbf{k}_{||}, \lambda)$ couples a SP mode and a reflected-wave mode specified by $\mathbf{k}_{||}$ and λ , respectively, and pertains to a given member of the random surface ensemble denoted by e . An explicit model^{4,6} of $V_e(\mathbf{k}_{||}, \lambda)$ and the form (2.5) are elaborated in Appendix A. In (2.5) and hereafter we abbreviate $\mathbf{k}_{||}$ by $||$ whenever possible to simplify the notation. The simple structure of (2.5) corresponds to the physical picture that a photon can be created, via the surface-roughness coupling, at the expense of one SP quanta and vice versa. As pointed out in the Introduction, we neglect in (2.5) terms of the form $\hat{a}_{\lambda}^{\dagger} \hat{a}_{\mu}$ and $\hat{a}_{\mathbf{k}_{||}}^{\dagger} \hat{a}_{\mathbf{q}_{||}}$ which represent “diffuse” scattering of light and SP, respectively, in keeping with the focus of this work on the light-SP coupling via the surface roughness.

The random nature of the surface profile $\zeta(\rho)$, (Fig. 1) is reflected in the properties of the matrix elements. For one, the subscript e in $V_e(\mathbf{k}_{||}, \lambda)$ indicates that for fixed $\mathbf{k}_{||}$ and λ , the matrix element is a random number over an ensemble e of surfaces. By the same token for a fixed ensemble member e , the matrix element $V_e(\mathbf{k}_{||}, \lambda)$ behaves erratically as a function of the surface-parallel components: For fixed $\mathbf{k}_{||}$ and \mathbf{k}_{λ} varying or for fixed \mathbf{k}_{λ} and $\mathbf{k}_{||}$ varying, the matrix element has a highly irregular behavior. The surface-parallel momentum component is singled out since a rough surface emits or absorbs *surface-parallel* momentum with a random amplitude. These features are explicitly borne out by the common surface-roughness model introduced by Elson and Ritchie⁶ (Appendix A). The structure of (2.5), however, is quite general. All subsequent manipulation depends only on this structure and the statistical properties of $V_e(\mathbf{k}_{||}, \lambda)$ just described and formulated in the next section.

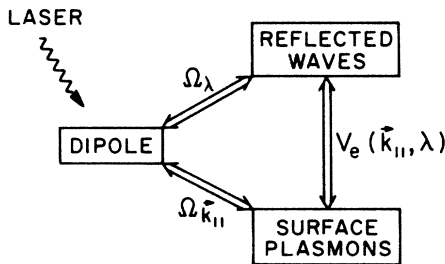


FIG. 2. Schematic flow chart of the couplings in the lossless rough metallic surface model. The notation for the coupling matrix elements is defined in the text. The driving laser, indicated by a wiggled arrow, is directed at the “dipole” box, to highlight the distinction between dynamic dipole–reflected-wave interaction (Ω_{λ}) and the dipole’s interaction with an extraneous driver.

III. THE EQUATIONS OF MOTION AND STATISTICAL ASSUMPTIONS

Our strategy is to solve the Heisenberg equations of motion corresponding to the Hamiltonian (2.5) in the weak driving-field limit, given the statistical assumptions on the SP-photon coupling $V_e(\mathbf{k}_{||}, \lambda)$ specified below.

Straightforward algebra yields the equations of motion:

$$\frac{d}{dt} \hat{B}(t) = -i\omega_D \hat{B}(t) - i \left[\sum_{\lambda} \Omega_{\lambda}^* \hat{a}_{\lambda}(t) + \sum_{\mathbf{k}_{||}} \Omega_{||}^* \hat{a}_{||}(t) \right], \quad (3.1a)$$

$$\frac{d}{dt} \hat{a}_{\lambda}(t) = -i\omega_{\lambda} \hat{a}_{\lambda}(t) - i\Omega_{\lambda} \hat{B}(t) - i \sum_{\mathbf{k}_{||}} V_e(\mathbf{k}_{||}, \lambda) \hat{a}_{||}(t), \quad (3.1b)$$

$$\frac{d}{dt} \hat{a}_{||}(t) = -i\omega_{||} \hat{a}_{||}(t) - i\Omega_{||} \hat{B}(t) - i \sum_{\lambda} V_e^*(\mathbf{k}_{||}, \lambda) \hat{a}_{\lambda}(t). \quad (3.1c)$$

The initial conditions at $t=0$ are that the atom is in its ground state $|0\rangle$ and the radiation field has no photons except in mode L of the weak continuous driving laser. The corresponding initial density matrix $\hat{\rho}_0$ is

$$\hat{\rho}_0 = |0\rangle \langle \alpha| \langle \alpha| \langle 0|, \quad (3.2)$$

such that the coherent state $|\alpha\rangle$ satisfies²⁴

$$\hat{a}_{\lambda} |\alpha\rangle = \delta_{\lambda, L} \alpha |\alpha\rangle. \quad (3.3)$$

For reasons that will become obvious shortly, we solve (3.1) by first eliminating $\hat{a}_{\lambda}(t)$ from (3.1c). Formally solving (3.1b) gives

$$\hat{a}_{\lambda}(t) = e^{-i\omega_{\lambda} t} \hat{a}_{\lambda} - i\Omega_{\lambda} \int_0^t d\tau e^{-i(\omega_{\lambda} - i\eta)(t-\tau)} \hat{B}(\tau) - i \sum_{\mathbf{q}_{||}} V_e(\mathbf{q}_{||}, \lambda) \int_0^t d\tau e^{-i(\omega_{\lambda} - i\eta)(t-\tau)} \hat{a}_{||}(\tau). \quad (3.4)$$

When the third term on the right-hand side of (3.4) is inserted into (3.1c) we are led to the following statistical assumptions (ϕ is an arbitrary smooth function):

$$\langle V_e(\mathbf{k}_{||}, \lambda) \rangle_e = 0, \quad (3.5a)$$

$$\sum_{\lambda} V_e^*(\mathbf{k}_{||}, \lambda) V_e(\mathbf{q}_{||}, \lambda) e^{-i\omega_{\lambda} t} = \delta_{\mathbf{k}_{||}, \mathbf{q}_{||}} \sum_{\lambda} |V_e(\mathbf{k}_{||}, \lambda)|^2 e^{-i\omega_{\lambda} t}, \quad (3.5b)$$

$$\sum_{\mathbf{k}_{||}} V_e(\mathbf{k}_{||}, \lambda) V_e^*(\mathbf{k}_{||}, \mu) \phi(\mathbf{k}_{||}) = \delta_{\mathbf{k}_{\lambda}, \mathbf{k}_{\mu}} \sum_{\mathbf{k}_{||}} V_e(\mathbf{k}_{||}, \lambda) V_e^*(\mathbf{k}_{||}, \mu) \phi(\mathbf{k}_{||}). \quad (3.5c)$$

The first equation (3.5a) is obvious. The δ factors in (3.5b) and (3.5c) are motivated by the statistical nature of the surface-parallel momentum transfer discussed in Sec. II: For fixed λ the $\mathbf{k}_{||}$ dependence of $V_e(\mathbf{k}_{||}, \lambda)$ has presumably a random phase [see, e.g., (A5)], and therefore the sum on the left-hand side of (3.5b) is dominated by the absolute squares; likewise for (3.5c). The statistical as-

sumptions (3.5) are at the basis of all subsequent derivations.

Note that would we try to eliminate $\hat{a}_{||}(t)$ from (3.1c) and insert it into (3.1b); the term corresponding to (3.5) would be

$$\sum_{\mathbf{k}_{||}} V_e(\mathbf{k}_{||}, \lambda) V_e^*(\mathbf{k}_{||}, \mu) e^{-i\omega_{||}t}.$$

This term, however, does *not* generate a $\delta_{\lambda, \mu}$ factor since the surface-perpendicular momenta components in λ and μ are not affected by the statistical nature of the surface roughness and hence can be different. Phrased differently, surface roughness *does* introduce correlations among reflected-wave modes with different q_λ , but sharing the same \mathbf{k}_λ . Consequently, although the equations of motion (3.1) are symmetric with respect to the reflected waves and SP modes, their solution given the statistical assumptions (3.5) is not, since surface roughness introduces randomness only in the surface-parallel momenta. The particular modeling of the surface roughness is included in the specifics of the matrix element $|V_e(\mathbf{k}_{||}, \lambda)|^2$.

With use of (3.4) and the statistical assumption (3.5b), insertion into (3.1c) yields (η is an infinitely small number)

$$\begin{aligned} \frac{d}{dt} \hat{a}_{||}(t) = & -i\omega_{||} \hat{a}_{||}(t) - i\Omega_{||} \hat{B}(t) - i \sum_{\lambda} V_e^*(\mathbf{k}_{||}, \lambda) e^{-i\omega_\lambda t} \hat{a}_\lambda \\ & - \sum_{\lambda} \Omega_\lambda V_e^*(\mathbf{k}_{||}, \lambda) \int_0^t d\tau e^{-i(\omega_\lambda - i\eta)(t-\tau)} \hat{B}(\tau) + \hat{J}(t), \end{aligned} \quad (3.6a)$$

$$\hat{J}(t) = - \sum_{\lambda} |V_e(\mathbf{k}_{||}, \lambda)|^2 \int_0^t d\tau e^{-i(\omega_\lambda - i\eta)(t-\tau)} \hat{a}_{||}(\tau). \quad (3.6b)$$

To solve (3.6) we invoke now the Markov-Born approximation twice.^{16,25} With regard to the $\hat{J}(t)$ term the justification is provided by the following argument. The λ summation includes summation over the surface-perpendicular momentum component. This induces an infinitely slow falloff, in ω_λ , of the matrix element $V_e(k_{||}, \lambda)$ [Eq. (A9)]. Therefore the function

$$J_1(t - \tau) = \sum_{\lambda} |V_e(k_{||}, \lambda)|^2 e^{-\omega_\lambda(t-\tau)}$$

is very sharply peaked in $t - \tau$, allowing us to approximate under the integral sign in (3.6b),

$$\hat{a}_{||}(\tau) = e^{-i\omega_{||}\tau} \hat{a}_{||}(\tau) \approx e^{-i\omega_{||}(\tau-t)} \hat{a}_{||}(t).$$

The same argument holds true for the term in (3.6a) involving the $\hat{B}(t)$ factor, since again the summation over the surface-perpendicular momentum component is non-statistical. Therefore in the Markov-Born approximation and the long-time limit, (3.6) takes the form

$$\begin{aligned} \frac{d}{dt} \hat{a}_{||}(t) = & -i(\omega_{||} - \delta_{||} - i\gamma_{||}) \hat{a}_{||}(t) \\ & - i[\Omega_{||} + f_e(\mathbf{k}_{||})] \hat{B}(t) + \hat{F}_R(\mathbf{k}_{||}, t), \end{aligned} \quad (3.7)$$

where

$$f_e(\mathbf{k}_{||}) = \sum_{\lambda} \Omega_\lambda V_e^*(\mathbf{k}_{||}, \lambda) \frac{1}{\omega_D - \omega_\lambda + i\eta} \quad (3.8)$$

and

$$\delta_{||} + i\gamma_{||} = - \sum_{\lambda} |V_e(\mathbf{k}_{||}, \lambda)|^2 \frac{1}{\omega_{||} - \omega_\lambda + i\eta} \quad (3.9)$$

with the surface-roughness noise term \hat{F}_R given by

$$\hat{F}_R(\mathbf{k}_{||}, t) = -i \sum_{\lambda} V_e^*(\mathbf{k}_{||}, \lambda) e^{-i\omega_\lambda t} \hat{a}_\lambda. \quad (3.10)$$

Equation (3.7) is interesting in several respects. (a) Note first that no “weak roughness” approximation has been invoked. Only the statistical properties of the matrix elements $V_e(\mathbf{k}_{||}, \lambda)$ were used. (b) Expression (3.9) (essentially the Fermi golden rule) yields the modified SP dispersion relation due to the surface roughness alone. This comment becomes obvious by considering the ensemble average of (3.7) [using (3.5a)] in the absence of a dipole^{8,21} ($\Omega_{||} = 0$). The additional correction to the SP dispersion relation due to dipole can be derived by inserting into (3.7) the solution for $\hat{B}(t)$ [Eq. (3.22)], and evaluating the proper Green function.²⁶ The corrections to the SP dispersion due to the diffuse light and SP scattering have been neglected from the outset, as discussed in the Introduction. (c) The static noise term $f_e(\mathbf{k}_{||})$ has a simple physical origin implied by its expression (3.8): It represents a process where the dipole emits a photon which then is reabsorbed by the rough surface and converted into a SP. This is a second channel for the dipole to create a SP, in addition to the direct coupling term $\Omega_{||}$. (d) The dynamic noise term \hat{F}_R , Eq. (3.10), is due to the direct SP-driving laser coupling (Fig. 2). It therefore enters a SP-driving term and gives (3.7) the appearance of a Langevin equation. In the presence of other uncorrelated noises, e.g., the optical Johnson noise, we expect additional additive terms (Sec. VI).

Before proceeding further we solve (3.7) formally by using again the Markov-Born approximation. The justification at this stage is similar to that employed for isolated atoms,^{16,25} i.e., typical $\omega_{||}$ and $\gamma_{||}$ are very large compared to the Rabi frequency associated with $\hat{B}(t)$. In the long-time limit ($\gamma_{||}t \gg 1$) this yields

$$\begin{aligned} \hat{a}_{||}(t) = & \frac{1}{\omega_D - \omega_{||} + i\gamma_R} [\Omega_{||} + f_e(\mathbf{k}_{||})] \hat{B}(t) \\ & + \sum_{\lambda} V_e^*(\mathbf{k}_{||}, \lambda) \frac{1}{\omega_\lambda - \omega_{||} + i\gamma_R} e^{-i\omega_\lambda t} \hat{a}_\lambda, \end{aligned} \quad (3.11)$$

where we used (3.10), and to simplify the notation we assumed

$$\delta_{||} + i\gamma_{||} \approx i\gamma_R = \text{const}. \quad (3.12)$$

Assumption (3.12) can be relaxed.

Similarly, by inserting (3.11) into (3.4) and using (3.5c), we obtain straightforwardly

$$\hat{a}_\lambda(t) = N_e(\lambda) e^{-i\omega_\lambda t} \hat{a}_\lambda - i[\Omega'_e(\lambda) + f_e(\lambda)] \times \int_0^t d\tau e^{-i(\omega_\lambda - i\eta)(t-\tau)} \hat{B}(\tau), \quad (3.13)$$

where

$$N_e(\lambda) = 1 + i\pi R(k_\lambda, q_\lambda) \sum_{\mathbf{q}_\parallel} |V_e(\mathbf{q}_\parallel, \lambda)|^2 \frac{1}{\omega_\parallel - \omega_\lambda - i\gamma_R},$$

$$\Omega'_e(\lambda) = \Omega_\lambda + i \sum_{\mathbf{q}_\parallel} V_e(\mathbf{q}_\parallel, \lambda) f_e(\mathbf{q}_\parallel) \frac{1}{\omega_\parallel - \omega_D - i\gamma_R}, \quad (3.14)$$

and

$$f_e(\lambda) = \sum_{\mathbf{q}_\parallel} V_e(\mathbf{q}_\parallel, \lambda) \Omega_\parallel \frac{1}{\omega_D - \omega_\parallel + i\gamma_R}. \quad (3.15)$$

The $R(k_\lambda, q_\lambda)$ factor in (3.14) is defined by $\delta_{k_\lambda, k_\mu} \int dq_\mu \delta(\omega_\lambda - \omega_\mu) = R(k_\lambda, q_\lambda)$ and we ignored—as throughout—principal value contributions.

Expression (3.13) separates explicitly the terms linear and bilinear in the fluctuating matrix elements $V_e(k_\parallel, \lambda)$. The bilinear terms are expected to fluctuate over the ensemble substantially less than the linear terms, particularly if a smoothing summation is involved such as in (3.14). We therefore approximate

$$N_e(\lambda) \approx \langle N_e(\lambda) \rangle_e = N_\lambda, \quad (3.16)$$

$$\Omega'_e(\lambda) \approx \langle \Omega'_e(\lambda) \rangle_e = \Omega'_\lambda,$$

and consequently

$$\hat{a}_\lambda(t) = N_\lambda e^{-i\omega_\lambda t} \hat{a}_\lambda - i[\Omega'_\lambda + f_e(\lambda)] \int_0^t d\tau e^{-i(\omega_\lambda - i\eta)(t-\tau)} \hat{B}(\tau). \quad (3.17)$$

At the expense of more complicated expressions (see below), approximations (3.16) can be relaxed.

With the aid of (3.11) and (3.17) the effective dipole operator equation is obtained by insertion into (3.1a) and invoking the Markov-Born approximation. The result is

$$\frac{d}{dt} \hat{B}(t) = -i(\omega_D - \Delta_D - i\gamma_D + f_e^c) \hat{B}(t) - \sum_\lambda \Omega_\lambda^* N_\lambda e^{i\omega_\lambda t} \hat{a}_\lambda - i \sum_{\mathbf{k}_\parallel} \Omega_\parallel^* \int_0^t d\tau e^{-i(\omega_\parallel - i\gamma_R)(t-\tau)} \hat{F}_R(\mathbf{k}_\parallel, \tau), \quad (3.18)$$

where

$$\Delta_D + i\gamma_D = \Delta_{\text{SP}} + i(\gamma_{\text{SP}} + \gamma_{\text{RW}}),$$

$$\Delta_{\text{SP}} + i\gamma_{\text{SP}} = - \sum_{\mathbf{k}_\parallel} |\Omega_\parallel|^2 \frac{1}{\omega_D - \omega_\parallel + i\gamma_R}, \quad (3.19)$$

$$\gamma_{\text{RW}} = \text{Re} \left[\pi \sum_\lambda \Omega_\lambda^* \Omega'_\lambda \delta(\omega_\lambda - \omega_D) \right],$$

and

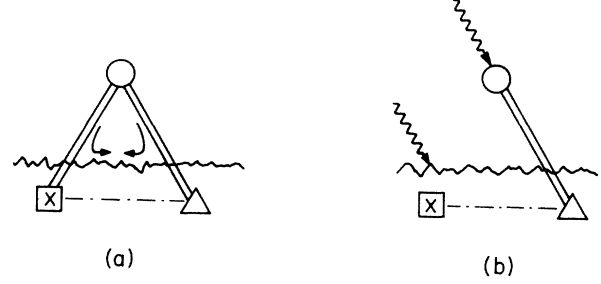


FIG. 3. Schematic representation of the roughness-induced terms in the dipole effective equation of motion (3.18). (a) represents the collisional noise term f_e^c (3.20). The dipole SP coupling (Ω_\parallel) and the dipole—reflected-wave coupling (Ω_λ) are indicated by two parallel lines, and the roughness-induced coupling V_e by a dashed-dotted line. The dipole is indicated by a circle, the SP modes and reflected-wave modes (photons) by a triangle and cross box, respectively. Thus (3a) depicts a process where the dipole emits a photon, which is converted by V_e into a SP, to couple back to the dipole. The same process in reverse is also contributing. (b) represents the driving terms in (3.20). The wiggled arrow stands for the driving laser. Using the same pictorial symbols as in (a), the extraneous laser can either directly drive the dipole, or create a SP via the intermediary of the rough surface, which drives the dipole.

$$f_e^c = \sum_{\mathbf{k}_\parallel} \frac{\Omega_\parallel^* f_e(\mathbf{k}_\parallel)}{\omega_D - \omega_\parallel + i\gamma_R} + \sum_\lambda \frac{\Omega_\lambda^* f_e(\lambda)}{\omega_D - \omega_\lambda + i\eta}$$

$$\approx -2\pi \sum_{\mathbf{k}_\parallel, \lambda} \frac{\text{Re}[\Omega_\lambda^* V_e(\mathbf{k}_\parallel, \lambda) \Omega_\parallel]}{(\omega_D - \omega_\parallel)^2 + \gamma_R^2} \delta(\omega_D - \omega_\lambda) \gamma_R. \quad (3.20)$$

The dipole operator equation of motion (3.18) is a key result of this work. The effect of surface roughness is to renormalize the widths and shifts and to introduce two noise terms, i.e., the “collisional noise” f_e^c and the additive driving-term noise which involves \hat{F}_R . The physical interpretation of these noise terms as suggested by (3.10) and (3.20) is the following: The collisional noise term represents a back-reaction of the dipole on itself [Fig. 3(a)]; the dipole emits a photon, which is converted into a SP by the surface roughness and then couples back to the dipole. The reverse route is also possible, hence the two terms in (3.20). The \hat{F}_R term [Fig. 3(b)] represents the contribution of driving the dipole by first converting a driving-laser photon into a SP quanta via the rough surface and the ensuing SP field drives the dipole. The f_e^c is time independent since only *elastic* scattering are mediated by the rough surface (in the long-time limit). The structure of (3.18) is identical to that encountered in the context of the optical Johnson noise,¹⁷ which makes it simple to combine the effect of the latter with surface roughness (Sec. VI).

The dipole operator equation of motion (3.18) can be formally solved, and upon insertion back into (3.11) and (3.17) it leads to a closed-form solution of the problem. These straightforward steps yield (in the long-time limit $t\gamma_D \gg 1$)

$$\hat{B}(t) = -i \sum_{\lambda} [N_{\lambda} \Omega_{\lambda}^* + f_e'(\lambda)] \hat{a}_{\lambda} e^{-i\omega_{\lambda} t} \int_0^t d\tau \exp[-i(\omega_D - \omega_{\lambda} - \Delta_D - i\gamma_D - f_e^c)(t - \tau)], \quad (3.21a)$$

where

$$f_e'(\lambda) = \sum_{\mathbf{q}_{\parallel}} V_e(\mathbf{q}_{\parallel}, \lambda) \Omega_{\parallel} \frac{1}{\omega_{\lambda} - \omega_{\parallel} + i\gamma_R}. \quad (3.21b)$$

Similarly

$$\hat{a}_{\parallel}(t) = \sum_{\lambda} e^{-i\omega_{\lambda} t} \hat{a}_{\lambda} \left[A_e(\lambda, \mathbf{k}_{\parallel}) + C_e(\lambda, \mathbf{k}_{\parallel}) \int_0^t d\tau \exp[-i(\omega_D - \omega_{\lambda} - \Delta_D - i\gamma_D + f_e^c)(t - \tau)] \right], \quad (3.22a)$$

where

$$A_e(\lambda, \mathbf{k}_{\parallel}) = V_e^*(\mathbf{k}_{\parallel}, \lambda) \frac{1}{\omega_{\lambda} - \omega_{\parallel} + i\gamma_R}, \quad (3.22b)$$

$$C_e(\lambda, \mathbf{k}_{\parallel}) = -i[\Omega_{\parallel} + f_e(\mathbf{k}_{\parallel})][N_{\lambda} \Omega_{\lambda}^* + f_e'(\lambda)] \frac{1}{\omega_D - \omega_{\parallel} + i\gamma_R}. \quad (3.22c)$$

Expressions (3.21) and (3.22) are the working relations for the next two sections. When sandwiched with (3.2) they imply that the dipole and SP respond with the driving laser frequency. Obviously, all the operator solutions depend on the particular ensemble-member index e either through a multiplicative factor, or the time integrals in (3.21)–(3.22).

IV. THE RESONANCE FLUORESCENCE SPECTRUM

The quantized-field formalism used hitherto is necessary to evaluate the effects of surface roughness on a dipole's resonance-fluorescence (RF) spectrum. The definition of the RF spectrum $S_{\text{RF}}(\omega_{\lambda})$ for a stationary system is²⁷

$$S_{\text{RF}}(\omega_{\lambda}) = \lim_{t \rightarrow \infty} \left[\frac{1}{t} \left\langle \left\langle i_{\text{RF}}(\omega_L) \left| \hat{a}_{\lambda}^{\dagger}(t) \hat{a}_{\lambda}(t) \right| i_{\text{RF}}(\omega_L) \right\rangle \right\rangle \right], \quad (4.1)$$

where the extra angular brackets in (4.1) denote an ensemble average and $|i_{\text{RF}}(\omega_L)\rangle$ corresponds to the initial density (3.2) with the weak driving laser of frequency ω_L . The mode λ in (4.1) is any reflected wave outside the specular direction. Inserting (3.17) into (4.1) gives

$$S_{\text{RF}}(\omega_{\lambda}) = \lim_{t \rightarrow \infty} \left[\left\langle \left\langle i_{\text{RF}}(\omega_L) \left| |\Omega'_{\lambda} + f_e(\lambda)|^2 \int_{-\infty}^{\infty} d\tau e^{i\omega_{\lambda}\tau} \hat{B}^{\dagger}(t - \tau) \hat{B}(t) \right| i_{\text{RF}}(\omega_L) \right\rangle \right\rangle \right], \quad (4.2)$$

which calls for the calculation of the dipole-dipole correlation function in the long-time limit.

To evaluate (4.2) we use (3.21) and (3.3). This yields

$$S_{\text{RF}}(\omega_{\lambda}) = |\alpha|^2 \delta(\omega_{\lambda} - \omega_L) \left\langle \left\langle |\Omega'_{\lambda} + f_e(\lambda)|^2 |N_{\lambda} \Omega_{\lambda}^* + f_e'(\lambda)|^2 \int_0^{\infty} dx \exp[i(\omega_D - \omega_L + i\gamma_D + f_e^c)x] \right. \right. \\ \left. \left. \times \int_0^{\infty} dy \exp[-i(\omega_D - \omega_L - i\gamma_D + f_e^c)y] \right\rangle \right\rangle, \quad (4.3)$$

where the dipole frequency shift Δ_D has been omitted for simplicity. The ensemble average implied in (4.3) can be easily carried out using the method outlined in Appendix B. The result is

$$S_{\text{RF}}(\omega_{\lambda}) = |\alpha|^2 \delta(\omega_{\lambda} - \omega_L) \left\{ \langle [|\Omega'_{\lambda} + f_e(\lambda)|^2][N_{\lambda} \Omega_{\lambda}^* + f_e'(\lambda)]^2 \rangle I_0(\omega_{\lambda} - \omega_L) \right. \\ \left. + \langle [|\Omega'_{\lambda} + f_e(\lambda)|^2][N_{\lambda} \Omega_{\lambda}^* + f_e'(\lambda)]^2 f_e^c \rangle I_1(\omega_{\lambda} - \omega_L) \right\}, \quad (4.4)$$

where [from Eqs. (B4) and (B5)]

$$I_0(\omega) = \int_0^{\infty} dx \int_0^{\infty} dy \exp[-i(\omega - i\gamma_D)x] \\ \times \exp[+i(\omega + i\gamma_D)y] \\ \times \exp[-\frac{1}{2}(x - y)^2 \gamma_c^2], \\ I_1(\omega) = \frac{d}{d\omega} I_0(\omega), \quad (4.5)$$

and

$$\gamma_c^2 = \langle (f_e^c)^2 \rangle. \quad (4.6)$$

Expressions (4.4)–(4.6) are the results of this section. The $\delta(\omega_{\lambda} - \omega_L)$ factor expresses the fact that in the absence of any source for *inelastic* scattering only the elastic scattering mediated by the surface roughness takes place. This is the Rayleigh δ peak. Surface roughness modifies the “line shape,” which is the ω -dependent multiplicative factors in (4.4). For an isolated dipole or a dipole near a flat surface (without Johnson noise) the line shape is a Lorentzian. In the presence of roughness the line shape is given by a combination of I_0 and I_1 , Eq. (4.4). The line shape I_0 has the following limiting forms:

$$I_0(\omega) \sim \begin{cases} \frac{1}{\omega^2 + \gamma_D^2} & \text{for } \gamma_D \gg \gamma_c, \\ \exp(-\omega^2/2\gamma_c^2) & \text{for } \gamma_D \ll \gamma_c. \end{cases} \quad (4.7)$$

The change of the line shape, from a Lorentzian to a Gaussian with the increase of the roughness-collisional width γ_c [Eq. (4.7)] is a central result of this work. We emphasize that this feature does not depend on the specific roughness model.

It is particularly interesting to estimate where both limits of (4.7) are realized. For this purpose we deduce from (3.19) and (3.20) the following order-of-magnitude estimates for the two widths involved:

$$\gamma_c \approx \rho [\Omega_{\parallel}] [\Omega_{\lambda}] \langle |V_e| \rangle, \quad (4.8)$$

and

$$\gamma_D \approx [|\Omega_{\parallel}|]^2 \rho + [|\Omega_{\lambda}|]^2 (1 + \langle V_e^2 \rangle \rho) \rho'. \quad (4.9)$$

In (4.8) and (4.9) the square brackets indicate a "typical" value of the matrix element and ρ, ρ' are uninteresting generic phase-space density factors. Expression (4.9) suggests the distinction between the regime when the dipole is "near" the surface, i.e., when the SP field dominates, and the regime when it is "far" from the surface when it is affected predominantly by the reflected waves. Consequently,

$$\gamma_D \approx \begin{cases} [|\Omega_{\parallel}|]^2 \rho & \text{for a "near" dipole,} \\ [|\Omega_{\lambda}|]^2 (1 + \langle V_e^2 \rangle \rho) \rho' & \text{for a "far" dipole.} \end{cases} \quad (4.10)$$

By juxtaposing (4.8) and (4.10) it is possible to analyze the two limits of (4.7). The Lorentzian limit, i.e., $\gamma_D \gg \gamma_c$, can be realized readily for both near and far dipole configurations. For a near dipole (4.8) and (4.10) yield $|\Omega_{\parallel}| \gg \rho |\Omega_{\lambda}| \langle |V_e| \rangle$. For a far dipole we distinguish between two situations. (a) In the "small" roughness limit, defined by $\langle V_e^2 \rangle \rho \ll 1$, comparing (4.8) and (4.10) yields $|\Omega_{\lambda}| \gg \rho |\Omega_{\parallel}| \langle |V_e| \rangle$. (b) In the "large" roughness limit, defined by $\langle V_e^2 \rangle \rho \gg 1$, the comparison of (4.8) and (4.10) gives $|\Omega_{\lambda}| \langle |V_e| \rangle \gg \rho |\Omega_{\parallel}|$. All these inequalities can be readily realized due to the fact that at small distances from the surface (within the SP field range) Ω_{\parallel} dominates, and at large distances it decays exponentially. Thus the Lorentzian limit is pervasive.

The Gaussian limit of (4.7) is more difficult to realize, if at all, according to the following considerations. For a near dipole, the condition $\gamma_D \ll \gamma_c$ implies, by using (4.8) and (4.10), that $|\Omega_{\parallel}| \ll \rho |\Omega_{\lambda}| \langle |V_e| \rangle$. However, the very definition of the near dipole regime as embodied

in (4.10) stipulates that $|\Omega_{\parallel}| \gg \rho |\Omega_{\lambda}| \langle |V_e| \rangle$, which is incompatible with the starting inequality. Hence we conclude that the Gaussian limit probably cannot be realized for a near dipole. For a far dipole we again distinguish between two situations. (a) In the small roughness limit, i.e., $\langle V_e^2 \rangle \rho \ll 1$, expressions (4.8) and (4.10) lead to $|\Omega_{\lambda}| \ll \rho |\Omega_{\parallel}| \langle |V_e| \rangle$. This inequality when combined with the definition of the far dipole regime as embodied in (4.10), i.e., $|\Omega_{\lambda}|^2 \gg |\Omega_{\parallel}|^2 \rho$, yields $\langle V_e^2 \rangle \rho \gg 1$, in contradiction to the starting hypothesis of small roughness. (b) In the large roughness limit, i.e., $\langle V_e^2 \rangle \rho \gg 1$, expressions (4.8) and (4.10) yield $|\Omega_{\lambda}| \langle |V_e| \rangle \rho \ll |\Omega_{\parallel}|$. On the other hand, the definition of the far dipole regime implies $|\Omega_{\lambda}|^2 \gg \rho |\Omega_{\parallel}|^2$, which, when combined with the above inequality yield $\langle V_e^2 \rangle \rho \ll 1$ in contradiction to the starting hypothesis.

The foregoing analysis can be summarized by the conclusion that the Lorentzian limit of (4.7) is almost always realized, whereas the Gaussian limit is not at all. This statement, however, does not rule out situations when $\gamma_c \approx \gamma_D$, characterized by a substantial distortion of a Lorentzian line shape.

V. THE ABSORPTION OR REFLECTIVITY SPECTRUM

The absorption spectrum is intimately connected to the reflectivity spectrum in the following way. Denote by $\Delta R(\omega_0)$ the deviation of the perturbed system (flat surface plus the roughness and an interacting dipole) reflectivity from that of the unperturbed system (flat surface and a noninteracting dipole), as a function of the probe-laser frequency ω_0 . Then²⁸

$$\Delta R(\omega_0) = \lim_{t \rightarrow \infty} \left[\frac{1}{i_0} \left\langle \left\langle \frac{\partial}{\partial t} \hat{H}_{\text{int}}^{(A)}(\text{probe laser, system}) \right\rangle \right\rangle \right], \quad (5.1)$$

where i_0 denotes the incoming flux (dimensionality: energy/[time \times (length)²]), and $\hat{H}_{\text{int}}^{(A)}(\text{probe laser, system})$ is the interaction per unit area. The extra angular brackets indicate ensemble average. The average in (5.1) is over the density matrix pertaining to the perturbed system and represents the average rate of flux removal from the specular direction by the perturbation. The connection to the absorption spectrum,^{3-6,14,17} defined as the rate of energy removal from the specular direction, is now derived.

In the present context (Fig. 1) the interaction Hamiltonian between the probe laser and the system, \hat{h}_{int} , and the related areal interaction density $\hat{H}_{\text{int}}^{(A)}$ are

$$\hat{h}_{\text{int}}(\text{probe laser, system}) = \hbar \Omega_0 (e^{-i\omega_L t} \hat{B}^\dagger + e^{+i\omega_L t} \hat{B}) + \hbar \sum_{\mathbf{k}_{\parallel}} [\alpha V_e^*(\mathbf{k}_{\parallel}, L) e^{-i\omega_L t} \hat{a}_{\parallel}^\dagger + \alpha^* V_e(\mathbf{k}_{\parallel}, L) e^{+i\omega_L t} \hat{a}_{\parallel}], \quad (5.2a)$$

and therefore

$$\hat{H}_{\text{int}}^{(A)}(\text{probe laser, system}) = \hbar \Omega_0 n (e^{-i\omega_L t} \hat{B}^\dagger + e^{+i\omega_L t} \hat{B}) + \hbar \sum_{\mathbf{k}_{\parallel}} [W_e^*(\mathbf{k}_{\parallel}) e^{-i\omega_L t} \hat{a}_{\parallel}^\dagger + W_e(\mathbf{k}_{\parallel}) e^{+i\omega_L t} \hat{a}_{\parallel}]. \quad (5.2b)$$

These expressions are obtained by considering the expectation value of (2.5) with a density matrix of the type (3.2). The new symbols in (5.2) are $\Omega_0 = \Omega_{\lambda=L}^* \alpha$ is the Rabi frequency (dimensionalities: 1/time), n is the areal density of the di-

poles [dimensionality: $1/(\text{length})^2$], and $W_e(\mathbf{k}_{\parallel}) = \alpha^* V_e(\mathbf{k}_{\parallel}, \lambda = L)/L^2$ (dimensionalities: α is $(\text{length})^{-1/2}$, $V_e(\mathbf{k}_{\parallel}, \lambda)$ is $(\text{length})^{1/2}/\text{time}$, $W_e(\mathbf{k}_{\parallel})$ is $1/[\text{time} \times (\text{length})^2]$). The second term on the right-hand side of (5.2b) represents the photon-SP coupling per unit area, which is the reason for the $1/L^2$ factor in $W_e(\mathbf{k}_{\parallel})$. This is in keeping with the quantization volume assumed throughout, i.e., an infinite rod with a square cross section of area L^2 . The subscript e in (5.2) is a reminder that at the end of the calculation and ensemble average must be taken.

Use of (5.2) in (5.1) in the linear response²⁸ (since the driving laser is weak) gives

$$\Delta R(\omega_0) = \frac{2\hbar\omega_0}{i_0} \left\{ \lim_{t \rightarrow \infty} \text{Re} \left[\left\langle \left\langle i_{AB} \left| \int_0^t d\tau e^{-i\omega_0\tau} \left[\Omega_0^2 n [\hat{B}(t-\tau), \hat{B}^\dagger(t)] + \sum_{\mathbf{k}_{\parallel}, \mathbf{q}_{\parallel}} L^2 W_e^*(\mathbf{q}_{\parallel}) W_e(\mathbf{k}_{\parallel}) [\hat{a}_{\mathbf{k}_{\parallel}}(t-\tau), \hat{a}_{\mathbf{q}_{\parallel}}^\dagger(t)] \right. \right. \right. \right. \right. \\ \left. \left. \left. + \Omega_0 n \sum_{\mathbf{k}_{\parallel}} L^2 W_e^*(\mathbf{k}_{\parallel}) [\hat{B}(t-\tau), \hat{a}_{\parallel}^\dagger(t)] \right. \right. \right. \\ \left. \left. \left. + \Omega_0 \sum_{\mathbf{k}_{\parallel}} W_e(\mathbf{k}_{\parallel}) [\hat{a}_{\parallel}(t-\tau), \hat{B}^\dagger(t)] \right| \left. \left. \left. \right. \right. \right] \right\}, \quad (5.3)$$

and $|i_{AB}\rangle$ is the initial state of the unperturbed system, i.e., the vacuum state of the radiation field and the two-level system in its ground state. In the absence of surface roughness, only the common first term on the right-hand side of (5.3) survives. In the other limit of the surface roughness only the second term in (5.3) contributes. Expression (5.3) is a generalization of these two limits.

To compute (5.3) we use the explicit expressions (3.21) and (3.22) and the results of Appendix B. The relevant correlation functions are

$$\lim_{t \rightarrow \infty} \lim_{t' \rightarrow \infty} \langle \langle i_{AB} | [\hat{B}(t), \hat{B}^\dagger(t')] | i_{AB} \rangle \rangle = \sum_{\lambda} e^{-i\omega_{\lambda}(t-t')} [\langle | \Omega_{\lambda} + f_e'(\lambda) |^2 \rangle I_0(\omega_D - \omega_{\lambda}) + \langle | \Omega_{\lambda} + f_e'(\lambda) |^2 f_e^c \rangle I_1(\omega_D - \omega_{\lambda})], \quad (5.4a)$$

$$\lim_{t \rightarrow \infty} \lim_{t' \rightarrow \infty} \langle \langle i_{AB} | X_e [\hat{a}_{\mathbf{k}_{\parallel}}(t), \hat{a}_{\mathbf{q}_{\parallel}}^\dagger(t')] | i_{AB} \rangle \rangle \\ = \sum_{\lambda} e^{-i\omega_{\lambda}(t-t')} \{ \langle X_e A_e(\lambda, \mathbf{k}_{\parallel}) A_e^*(\lambda, \mathbf{q}_{\parallel}) \rangle + \langle X_e B_e(\lambda, \mathbf{k}_{\parallel}) B_e^*(\lambda, \mathbf{q}_{\parallel}) \rangle I_0(\omega_D - \omega_{\lambda}) \\ + \langle X_e B_e(\lambda, \mathbf{k}_{\parallel}) B_e^*(\lambda, \mathbf{q}_{\parallel}) f_e^c \rangle I_1(\omega_{\lambda} - \omega_D) + 2 \text{Re} [\langle X_e A_e(\lambda, \mathbf{k}_{\parallel}) B_e^*(\lambda, \mathbf{q}_{\parallel}) \rangle I_2^*(\omega_D - \omega_{\lambda}) \\ + \langle X_e A_e(\lambda, \mathbf{k}_{\parallel}) B_e^*(\lambda, \mathbf{q}_{\parallel}) f_e^c \rangle I_3^*(\omega_D - \omega_{\lambda})] \}, \quad (5.4b)$$

and

$$\lim_{t \rightarrow \infty} \lim_{t' \rightarrow \infty} \langle \langle i_{AB} | X_e [\hat{B}(t), \hat{a}_{\mathbf{k}_{\parallel}}^\dagger(t')] | i_{AB} \rangle \rangle \\ = \sum_{\lambda} e^{-i\omega_{\lambda}(t-t')} \{ \langle X_e [\Omega_{\lambda}^* + f_e'^*(\lambda)] A_e^*(\lambda, \mathbf{k}_{\parallel}) \rangle I_2(\omega_D - \omega_{\lambda}) + \langle X_e [\Omega_{\lambda}^* + f_e'^*(\lambda)] A_e^*(\lambda, \mathbf{k}_{\parallel}) f_e^c \rangle I_3(\omega_D - \omega_{\lambda}) \\ + \langle X_e [\Omega_{\lambda}^* + f_e'^*(\lambda)] B_e(\lambda, \mathbf{k}_{\parallel}) \rangle I_0(\omega_D - \omega_{\lambda}) + \langle X_e [\Omega_{\lambda}^* + f_e'^*(\lambda)] B_e(\lambda, \mathbf{k}_{\parallel}) f_e^c \rangle I_1(\omega_D - \omega_{\lambda}) \}. \quad (5.4c)$$

In (5.4), X_e denotes an arbitrary random variable over the ensemble and from [(B6) and (B7)]

$$I_2(\omega) = \frac{1}{\gamma_c} \left[\frac{\pi}{2} \right]^{1/2} \exp[-(\omega - i\gamma_c)^2 / 2\gamma_c^2], \quad (5.5) \\ I_3(\omega) = \frac{d}{d\omega} I_2(\omega).$$

Expressions (5.4) when inserted into (5.3) yield the central result of this section. As it is evident, the general line shape is quite complex since the ω_{λ} dependence [the time integral in (5.3) yields trivially $\omega_{\lambda} = \omega_0$] resides in the $I_i(\omega)$ integrals and the various averages over the ensemble. The discussion of the lineshape is deferred to a later publication. Note again that Eqs. (5.3)–(5.4) are valid for an arbitrary roughness amplitude.

We conclude this section by considering a special limit of (5.3), i.e., when no dipoles exist. In this limit only the $\langle [\hat{a}_{\mathbf{k}_{\parallel}}(t), \hat{a}_{\mathbf{q}_{\parallel}}^\dagger(t')] X_e \rangle$ correlation contributes with the result:

$$\Delta R(\omega_0) = \frac{2\hbar\omega_0}{i_0} \sum_{\lambda} \sum_{\mathbf{k}_{\parallel}} \frac{\langle L^2 | W_e(\mathbf{k}_{\parallel}) |^2 | V_e(\mathbf{k}_{\parallel}, \lambda) |^2 \rangle \delta(\omega_{\lambda} - \omega_0)}{(\omega_0 - \omega_{\parallel})^2 + \gamma_R^2}. \quad (5.6)$$

This results suggests a peak²² around $\omega_0 \sim \omega_{SP} = \omega_p / \sqrt{2}$ due the preponderance of SP modes around the asymptotic SP energy¹⁷ ω_{SP} . The width of the peak is the larger of γ_R or σ , where σ (Appendix A) pertains to $\langle |V_e|^2 \rangle$ and denotes the roughness correlation function.

VI. THE ADDITION OF OHMIC-LOSS EFFECTS AND DISCUSSION

The model discussed so far assumes, for the sake of simplicity, that the surface is lossless. This assumption is now relaxed to account for the Ohmic losses and the accompanying optical Johnson noise.¹⁷ To achieve this we introduce a coupling between the SP modes and a “statistical bath,” along the lines of the reservoir-theory ansatz^{17,29} (Fig. 4). This (boson) bath represents the random currents arising from inelastic collisions between the SP charge-wave modes and lattice imperfections. This physical picture is in keeping with the Drude model of metallic conductivity. Accordingly, Eq. (3.1c) is replaced by the following two equations:

$$\frac{d}{dt} \hat{O}_{\beta}(t) = -i\omega_{\beta} \hat{O}_{\beta}(t) - i \sum_{\mathbf{k}_{\parallel}} g(\mathbf{k}_{\parallel}, \beta) \hat{a}_{\parallel}(t), \quad (6.1a)$$

$$\begin{aligned} \frac{d}{dt} \hat{a}_{\parallel}(t) &= -i\omega_{\parallel} \hat{a}_{\parallel}(t) - i\Omega_{\parallel} \hat{B}(t) \\ &\quad - i \sum_{\lambda} V_e^*(\mathbf{k}_{\parallel}, \lambda) \hat{a}_{\lambda}(t) - i \sum_{\beta} g^*(\mathbf{k}_{\parallel}, \beta) \hat{O}_{\beta}(t), \end{aligned} \quad (6.1b)$$

where $\hat{O}_{\beta}^{\dagger}$ creates a quanta of bath mode β and $g(\mathbf{k}_{\parallel}, \beta)$ is the coupling matrix element between a SP mode specified

$$\begin{aligned} \frac{d}{dt} \hat{B}(t) &= -i(\omega_D - \Delta_D - i\gamma_D + f_e^c) \hat{B}(t) - i \sum_{\lambda} N_{\lambda} \Omega_{\lambda}^* e^{-i\omega_{\lambda} t} \hat{a}_{\lambda} - i \sum_{\mathbf{k}_{\parallel}} \Omega_{\parallel}^* \int_0^t d\tau e^{-i(\omega_{\parallel} - i\gamma_T)(t-\tau)} [\hat{F}_R(\mathbf{k}_{\parallel}, \tau) + \hat{F}_J(\mathbf{k}_{\parallel}, \tau)] \\ &\quad - i \sum_{\lambda} \Omega_{\lambda}^* \sum_{\mathbf{q}_{\parallel}} V_e(\mathbf{q}_{\parallel}, \lambda) \int_0^t d\tau e^{-i(\omega_{\lambda} - i\eta)(t-\tau)} \int_0^{\tau} d\tau' e^{-i(\omega_{\parallel} - i\gamma_T)(\tau-\tau')} \hat{F}_J(\mathbf{q}_{\parallel}, \tau') \end{aligned} \quad (6.4)$$

and

$$\begin{aligned} \hat{a}_{\lambda}(t) &= N_{\lambda} e^{-i\omega_{\lambda} t} \hat{a}_{\lambda} - i[\Omega'(\lambda) + f_e(\lambda)] \int_0^t d\tau e^{-i(\omega_{\lambda} - i\eta)(t-\tau)} \hat{B}(\tau) \\ &\quad - i \sum_{\mathbf{q}_{\parallel}} V_e(\mathbf{q}_{\parallel}, \lambda) \int_0^t d\tau e^{-i(\omega_{\lambda} - i\eta)(t-\tau)} \int_0^{\tau} d\tau' e^{-i(\omega_{\parallel} - i\gamma_T)(\tau-\tau')} \hat{F}_J(\mathbf{q}_{\parallel}, \tau'). \end{aligned} \quad (6.5)$$

In (6.4) and (6.5) we denote $\gamma_T = \gamma_R + \gamma_J$, and the dipole's total frequency shift and broadening Δ_D and γ_D are obtained from (3.19) by substituting $\gamma_R \rightarrow \gamma_T$. The interesting terms in (6.4) and (6.5) are those which involve a *product* of the two noises $V_e(\mathbf{q}_{\parallel}, \lambda)$ and $\hat{F}_J(\mathbf{k}_{\parallel}, t)$. These can be neglected in the (common) limit of either weak roughness or weak optical Johnson noise, in which case, apart from f_e^c , the roughness and the optical Johnson noises add incoherently.

The RF and absorption spectra ensuing from

by \mathbf{k}_{\parallel} and bath mode β . The statistical properties of the $g(\mathbf{k}_{\parallel}, \beta)$ are articulated elsewhere,¹⁷ and we assume that $\langle \hat{O}_{\beta}(t=0) \hat{O}_{\alpha}(t=0) \rangle = \delta_{\alpha\beta} n_{\beta}(T)$ where T is the bath temperature and $n_{\beta}(T)$ is the occupation number.

The next step is to solve the augmented set of equations of motion [Eqs. (3.1a), (3.1b), and (6.1)]. Following the steps discussed in Sec. III, the result for the SP equation of motion is

$$\begin{aligned} \frac{d}{dt} \hat{a}_{\parallel}(t) &= -i[\omega_{\parallel} - i(\gamma_R + \gamma_J)] \hat{a}_{\parallel}(t) - i[\Omega_{\parallel} + f_e(\mathbf{k}_{\parallel})] \hat{B}(t) \\ &\quad + \hat{F}_R(\mathbf{k}_{\parallel}, t) + \hat{F}_J(\mathbf{k}_{\parallel}, t), \end{aligned} \quad (6.2)$$

where the optical Johnson noise $\hat{F}_J(\mathbf{k}_{\parallel}, t)$ is given by¹⁷

$$\hat{F}_J(\mathbf{k}_{\parallel}, t) = -i \sum_{\beta} g^*(\mathbf{k}_{\parallel}, \beta) e^{-i\omega_{\beta} t} \hat{O}_{\beta}, \quad (6.3)$$

and the approximately constant Johnson noise SP broadening is γ_J [see Ref. 17, Eq. (2.11)]. Comparing (6.2) with (3.7), and (6.3) with (3.10), we see the similarity in *structure* between the optical Johnson noise and the surface-roughness terms. Equation (3.4) is still valid, since only the SP modes are assumed to couple to the “bath” (Fig. 4).

The effective dipole operator equation of motion can now be derived in a straightforward manner. The result is

(6.2)–(6.5) can be worked out using (4.1) and (5.3). Obviously the predicted line shapes are rather complex and are not discussed here any further. The expected qualitative features, however, can be discussed in terms of the features exhibited separately by the spectra corresponding to the optical Johnson noise¹⁷ and surface roughness. For instance, the RF spectrum is expected to contain, besides the Rayleigh peak and the resonance fluorescence peak around ω_D ,³⁰ an additional broad peak centered around ω_{SP} , the asymptotic SP frequency. The line shapes are ex-

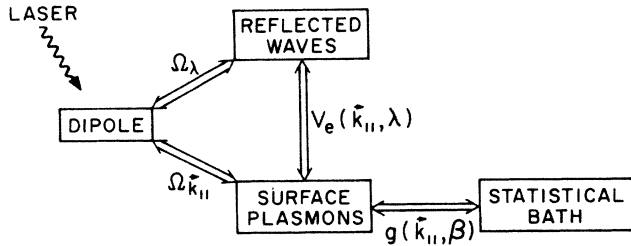


FIG. 4. The schematic flow chart of the extended model, Eq. (6.1), including Ohmic-loss effects. Compare with Fig. 2. The coupling matrix elements are defined in the text and the extraneous driving laser is indicated by a wiggled arrow.

pected to deviate from a Lorentzian, or a product of Lorentzians, toward Gaussian-type shapes whenever the roughness amplitude is large enough.

To summarize, we have analyzed the effects of random metallic surface roughness on light scattering from a nearby dipole in terms independent of the details of the roughness model. The analysis is confined to the weak driving-laser field laser and to the discussion of the resonance fluorescence and reflectivity spectra. Our model accounts for the coupling of light to the SP excitation through the intermediary of the surface roughness of arbitrary amplitude, while neglecting for the sake of simplicity, the “diffuse” light and SP scattering by the surface roughness. The inclusion of the latter scattering processes introduces substantial complications and is deferred to another publication.

A novel feature of our approach is the use of a fully quantum-mechanical formulation. One advantage of this approach is that it leads naturally to the discussion of surface-roughness effects in terms of the matrix elements that couple photons and SP modes. The random character of the surface profile is reflected in the simple statistical properties of these matrix elements. This vantage point appeals to us as very intuitive. It transcends the specifics of any particular roughness model and neatly includes the ignorance about what a rough surface really is into well-defined phenomenological parameters, e.g., γ_c . Our framework also lends itself to a complete dynamical solution of the model which may prove useful in future applications, e.g., the study of modified SP dispersion relations.

The main result of this work, besides establishing the usefulness of a quantum-mechanical formalism, is the new roughness-induced line shapes of the resonance fluorescence and absorption spectra. The RF line shape is distorted away from a Lorentzian shape toward a Gaussian shape with an increase of the roughness amplitude. This result hinges only on the statistical assumptions of the matrix elements mentioned above. Another interesting result is the discussion of the coexistence of surface roughness and the optical Johnson noise. The ensuing line shapes are quite complex, but can crudely be described as “distorted Lorentzian peaks centered around the RF frequency ω_D and the asymptotic SP frequency ω_{SP} .”

Our results with regard to line shapes call for an experi-

mental test with well-characterized rough surfaces.

ACKNOWLEDGMENTS

I would like to thank Professor D. G. Hall for many stimulating discussions. This work has been supported by the U.S. Air Force Office of Scientific Research, under Contract No. AFOSR-81-0204-A.

APPENDIX A: THE ELSON-RITCHIE MODEL FOR ROUGHNESS-INDUCED COUPLING

The surface-roughness model of Elson and Ritchie⁶ provides a useful guideline for the statistical assumptions employed in our approach. For this reason it is recapitulated below, using the notation of this work.

The interaction Hamiltonian is of the type $\Delta \mathbf{j} \cdot \mathbf{A}$, where the access current $\Delta \mathbf{j}$ originates from the deviations of electron density in a rough surface as compared to that of a flat surface and \mathbf{A} is the electromagnetic potential. Therefore

$$H_{\text{int}} = \frac{|e|}{c} \int dv [n(\mathbf{r}) - n_0 \Theta(-z)] \mathbf{A}_\lambda(\mathbf{r}) \cdot \mathbf{v}_{\text{SP}}(\mathbf{r}),$$

$$n(\mathbf{r}) = n_0 \Theta(-z - \zeta_e(\rho)). \quad (\text{A1})$$

In (A1), n_0 is the constant electron density, terminating abruptly at the surface located at $z=0$ (Fig. 1), $\zeta_e(\rho)$ is the random deviation of the surface profile from that of a perfectly flat surface, \mathbf{A}_λ is the reflected waves electromagnetic potential, $\mathbf{v}_{\text{SP}}(\mathbf{r})$ is the velocity of the SP charge wave, $|e|$ is the electric charge (in Gaussian units), c is the speed of light, and Θ is the step functions.

In the “small” roughness limit we expand (A1) to first order in $\zeta_e(\rho)$

$$n(\mathbf{r}) - n_0 \Theta(-z) \cong -n_0 \zeta_e(\rho) \delta(z). \quad (\text{A2})$$

Consequently the quantized interaction term takes the form

$$\hat{H}_{\text{int}} = -\frac{|e|}{c} n_0 \int d\rho \zeta_e(\rho) \hat{\mathbf{A}}_\lambda(\rho; z=0) \cdot \hat{\mathbf{v}}_{\text{SP}}(\rho; z=0), \quad (\text{A3})$$

where the quantization volume, as throughout, is an infinite rod with a square cross section of area L^2 . By inserting the spectral mode expansions of $\hat{\mathbf{A}}_\lambda$ and $\hat{\mathbf{v}}_{\text{SP}}^4$ into (A3), we recover the form (2.4). Note that at this point we neglected the antiresonant terms.¹⁶ Inserting the full electromagnetic potential into (A3) would give rise to a term describing the (“diffuse”) SP-SP scattering due to the surface roughness.

To complete the model, the statistical assumptions for the stochastic variable $\zeta_e(\rho)$ are now specified. They are

$$\langle \zeta_e(\rho) \rangle_e = 0,$$

$$\langle \zeta_e(\rho) \zeta_e(\rho') \rangle_e = \Delta^2 W(|\rho - \rho'|), \quad (\text{A4})$$

where Δ is the root-mean-square deviation of the roughness height and $W(|\rho|)$ is a dimensionless correlation

function. For a popular choice⁴ $W(|\rho|) = \exp(-\rho^2/\sigma^2)$, typical values of the parameters⁶ are $\sigma \approx 200-1000 \text{ \AA}$ and $\Delta \approx 10-100 \text{ \AA}$. The model defined by (A3)–(A4) implies the following matrix elements:

$$V_e(\mathbf{k}_{\parallel}, \lambda) = \frac{1}{L^2} C_R A_e(\mathbf{k}_{\parallel} - \mathbf{k}_{\lambda}) Y(k_{\parallel}) Z(k_{\lambda}, q_{\lambda}), \quad (\text{A5})$$

where

$$\begin{aligned} C_R &= -\frac{|e|}{\hbar c} n_0 i \left[\frac{4\hbar c^2}{m n_0} \right]^{1/2}, \\ A_e(\mathbf{k}_{\parallel} - \mathbf{k}_{\lambda}) &= \int d\rho \xi_e(\rho) e^{i(\mathbf{k}_{\parallel} - \mathbf{k}_{\lambda}) \cdot \rho}, \\ \nu(k_{\parallel}) &= (-W_1^2)^{1/2}, \\ Y(k_{\parallel}) &= \left[\frac{\hbar \omega(k_{\parallel}) \nu(k_{\parallel}) k_{\parallel}^4}{\nu^4(k_{\parallel}) + k_{\parallel}^4} \right]^{1/2} \frac{\nu^4(k_{\parallel})}{k_{\parallel}}, \\ Z(k_{\lambda}, q_{\lambda}) &= \left[\frac{c^2 q_{\lambda}^2}{\omega(k_{\lambda}, q_{\lambda})^3} \right]^{1/2} \left[\frac{-W_1^2}{-W_1^2 + \epsilon_1 W_0^2} \right]^{1/2}, \end{aligned} \quad (\text{A6})$$

and we used $W_i = (\epsilon_i k_0^2 - k_{\parallel}^2)^{1/2}$ where $i=0$ is air and $i=1$ is the dielectric, $k_0 = \omega_0/c$, $\omega(k_{\lambda}, q_{\lambda}) = c(k_{\lambda}^2 + q_{\lambda}^2)^{1/2}$, and m is the electron mass. The dimensionality of $V_e(\mathbf{k}_{\parallel}, \lambda)$ is (length)^{1/2}/time. Finally the ensemble average of a product of two matrix elements gives

$$\begin{aligned} \langle V_e(\mathbf{k}_{\parallel}, \lambda) V_e^*(\mathbf{q}_{\parallel}, \mu) \rangle &= \frac{1}{L^2} |C_R|^2 \Delta^2 \delta_{\mathbf{k}_{\parallel} - \mathbf{q}_{\parallel} - \mathbf{k}_{\lambda} + \mathbf{k}_{\mu}} \\ &\times W(|\mathbf{k}_{\parallel} + \mathbf{q}_{\parallel} - \mathbf{k}_{\lambda} - \mathbf{k}_{\mu}|) \\ &\times Y(k_{\parallel}) Y(q_{\parallel}) \\ &\times Z(k_{\lambda}, q_{\lambda}) Z(k_{\mu}, q_{\mu}), \end{aligned} \quad (\text{A7})$$

and $W(|k|)$ is the two-dimensional Fourier transform of $W(|\rho|)$. For the above-mentioned Gaussian ansatz of $W(|\rho|)$ the expression is

$$w(2k) = \pi \sigma^2 e^{-\sigma^2 k^2/4}. \quad (\text{A8})$$

Expressions (A5) and (A7) highlight the distinction between the dependencies on the surface-parallel and surface-perpendicular momenta. In fact, since

$$Z(k_{\lambda}, q_{\lambda}) \rightarrow q_{\lambda}^{-1/2} \sim \omega_{\lambda}^{-1} \text{ as } q_{\lambda}/k_{\lambda} \rightarrow \infty, \quad (\text{A9})$$

the matrix element (A5), or the correlation function (A7) are very (infinitely) broad in the ω_{λ} variable. The surface-parallel momenta exchange, on the other hand, is constrained by momentum conservation and the surface correlation length σ^{-1} . These features motivate the statistical assumptions (3.5).

APPENDIX B: ENSEMBLE AVERAGES

All the necessary ensemble averages can be evaluated by use of the following general theorem³¹ for Gaussian stochastic variables $\xi(\theta)$ with vanishing average:

$$\left\langle \exp \left[i \int_{-\infty}^{\infty} d\theta J(\theta) \xi(\theta) \right] \right\rangle = \exp \left[-\frac{1}{2} \int_{-\infty}^{\infty} d\tau_1 \int_{-\infty}^{\infty} d\tau_2 J(\tau_1) J(\tau_2) \langle \xi(\tau_1) \xi(\tau_2) \rangle \right] \quad (\text{B1})$$

and $J(\theta)$ is an arbitrary function. It follows therefore that

$$\langle \exp(itf_e^c) \rangle = \exp \left[-\frac{t^2}{2} \gamma_c^2 \right], \quad (\text{B2})$$

$$\langle X_e \exp(-itf_e^c) \rangle = \langle X_e \rangle \langle \exp(-itf_e^c) \rangle - it \langle X_e f_e^c \rangle \exp \left[-\frac{t^2}{2} \gamma_c^2 \right],$$

where X_e is an arbitrary Gaussian random variable and

$$\gamma_c^2 = \langle (f_e^c)^2 \rangle. \quad (\text{B3})$$

Using (B2) the following simple expressions follow:

$$\begin{aligned} I_0(\omega_D - \omega_{\lambda}) &= \left\langle \int_0^{\infty} dx \exp[-i(\omega_D - \omega_{\lambda} - i\gamma_D + f_e^c)x] \int_0^{\infty} dy \exp[+i(\omega_D - \omega_{\lambda} + i\gamma_D + f_e^c)y] \right\rangle \\ &= \int_0^{\infty} dx \int_0^{\infty} dy \exp[-i(\omega_D - \omega_{\lambda} - i\gamma_D)x] \exp[+i(\omega_D - \omega_{\lambda} + i\gamma_D)y] \exp[-\frac{1}{2}(x-y)^2 \gamma_c^2], \end{aligned} \quad (\text{B4})$$

$$\left\langle X_e \int_0^{\infty} dx [-i(\omega_D - \omega_{\lambda} - i\gamma_D + f_e^c)x] \int_0^{\infty} dy \exp[+i(\omega_D - \omega_{\lambda} + i\gamma_D + f_e^c)y] \right\rangle = \langle X_e \rangle I_0(\omega_D - \omega_{\lambda}) + \langle X_e f_e^c \rangle I_1(\omega_D - \omega_{\lambda}), \quad (\text{B5})$$

$$I_1(\omega_D - \omega_{\lambda}) = \frac{d}{d(\omega_D - \omega_{\lambda})} I_0(\omega_D - \omega_{\lambda}),$$

$$I_2(\omega_D - \omega_{\lambda}) = \left\langle \int_0^{\infty} dx \exp[-i(\omega_D - \omega_{\lambda} - i\gamma_D + f_e^c)x] \right\rangle = \frac{1}{\gamma_c} \left[\frac{\pi}{2} \right]^{1/2} \exp[-(\omega_D - \omega_{\lambda} - i\gamma_c)^2/2\gamma_c^2], \quad (\text{B6})$$

$$\left\langle X_e \int_0^\infty dx \exp[-i(\omega_D - \omega_\lambda - i\gamma_D + f_e^c)x] \right\rangle = \langle X_e \rangle I_2(\omega_D - \omega_\lambda) + \langle X_e f_e^c \rangle I_3(\omega_D - \omega_\lambda),$$

$$I_3(\omega_D - \omega_\lambda) = \frac{d}{d(\omega_D - \omega_\lambda)} I_2(\omega_D - \omega_\lambda). \quad (\text{B7})$$

The analytic form of $I_0(\omega_D - \omega_\lambda)$ in two interesting limits is discussed in the text.

*Present address: Naval Surface Weapons Center, White Oak Laboratory, Silver Spring, MD 20903-5000.

¹A. recent comprehensive review is A. A. Maradudin, in *Surface Polaritons*, edited by V. M. Agranovich and D. L. Mills (North-Holland, New York, 1982), p. 405.

²See, for instance, A. Wokaun, in *Solid State Physics*, edited by H. Ehrenrich and D. Trunbull (Academic, New York, 1984), Vol. 38, p. 224.

³R. H. Ritchie and R. E. Wilems, *Phys. Rev.* **178**, 372 (1968).

⁴J. Crowell and R. H. Ritchie, *J. Opt. Soc. Am.* **60**, 795 (1970).

⁵J. M. Elson and R. H. Ritchie, *Phys. Lett.* **33A**, 255 (1970).

⁶J. M. Elson and R. H. Ritchie, *Phys. Rev. B* **4**, 4129 (1971).

⁷P. K. Hansma and H. P. Broida, *App. Phys. Lett.* **32**, 545 (1978); J. R. Kirtley, T. N. Thies, J. C. Tang, and D. J. Dimaria, *Phys. Rev. B* **27**, 4601 (1983).

⁸B. Laks and D. L. Mills, *Phys. Rev. B* **20**, 4962 (1978); **21**, 5175 (1980).

⁹R. W. Rendell and D. J. Scalapino, *Phys. Rev. B* **24**, 3276 (1981).

¹⁰Representative references are A. A. Maradudin and D. L. Mills, *Phys. Rev. B* **11**, 1392 (1976); G. A. Farias and A. A. Maradudin, *ibid.* **28**, 5675 (1983); K. Arya, *ibid.* **30**, 7242 (1984).

¹¹G. Brown, V. Celli, M. Haller, A. A. Maradudin, and A. Marvin, *Phys. Rev. B* **31**, 4993 (1985).

¹²J. E. Sipe, J. F. Young, J. S. Preston, and H. M. Van Driel, *Phys. Rev. B* **27**, 1141 (1983); J. E. Sipe, H. M. Van Driel, and J. Young, *Can. J. Phys.* **63**, 104 (1985).

¹³G. S. Agarwal, *Phys. Rev. B* **15**, 2371 (1977).

¹⁴V. Celli, A. Marvin, and F. Toigo, *Phys. Rev. B* **11**, 1779 (1975); A. Marvin, F. Toigo, and V. Celli, *ibid.* **11**, 2777 (1975); F. Toigo, A. Marvin, V. Celli, and N. R. Hill, *ibid.* **15**, 5618 (1977).

¹⁵G. W. Ford and W. H. Weber, *Phys. Rep.* **113**, 195 (1984).

¹⁶L. Allen and J. H. Eberly, *Optical Resonance and Two Level Atoms* (Wiley, New York, 1975), Chap. 7.

¹⁷D. Agassi and J. H. Eberly, *Phys. Rev. Lett.* **54**, 34 (1985); D. Agassi, *Phys. Rev. B* **32**, 7835 (1985).

¹⁸*Laser Speckle and Related Phenomena*, edited by J. C. Dainty (Springer-Verlag, Berlin, 1975).

¹⁹D. L. Mills, *Phys. Rev. B* **12**, 4036 (1975); A. A. Maradudin and W. Zierau, *ibid.* **14**, 484 (1976).

²⁰E. Kretschmann, T. L. Ferrell, and J. C. Ashley, *Phys. Rev.* **19**, 1312 (1979).

²¹D. G. Hall and A. J. Baundmeier, Jr., *Phys. Rev. B* **17**, 3808 (1978).

²²S. N. Jasperson and S. E. Schnatterly, *Phys. Rev.* **188**, 759 (1978); L. J. Cunningham and A. J. Braundmeier, *ibid.* **14**, 479 (1976).

²³X. Y. Huang, H. Lin, and T. F. George, *J. Chem. Phys.* **80**, 893 (1984); X. Y. Huang and T. F. George, *J. Phys. Chem.* **88**, 4801 (1984).

²⁴R. Loudon, *The Quantum Theory of Light* 2nd ed. (Oxford, London 1983).

²⁵J. D. Cresser, Ph.D. thesis, University of Queensland, St. Lucia, Queensland, 1979 (unpublished).

²⁶S. Doniach and E. H. Sondheimer, *Green's Functions for Solid State Physicists* (Benjamin, Reading, 1974), p. 150.

²⁷B. R. Mollow, *Phys. Rev.* **188**, 1969 (1969).

²⁸B. R. Mollow, *Phys. Rev. A* **5**, 1522 (1972); B. J. Dalton, in *Coherence and Quantum Optics V*, edited by L. Mandel and E. Wolf (Plenum, New York, 1984), p. 781.

²⁹M. Sargent III, M. O. Scully, and W. E. Lamb, *Laser Physics* (Addison-Wesley, Reading, 1974), Chap. XIX.

³⁰Reference 24, Sec. 8.2.

³¹See for example, A. Papoulis, *Probability, Random Variables and Stochastic Processes* (McGraw-Hill, New York, 1965); K. Wodkiewicz, *Phys. Rev. A* **19**, 1686 (1979).